
Paper:
Tang, K. (in press). Effects of water column processes on the use of sediment traps to measure zooplankton non-predatory mortality: a mathematical and empirical assessment. *Journal of Plankton Research*

Effects of water column processes on the use of sediment traps to measure zooplankton non-predatory mortality: a mathematical and empirical assessment

Olga P. Dubovskaya[1,2*], Aleksandr P. Tolomeev[1], Georgiy Kirillin[3], Zhanna Buseva[4], Kam W. Tang[5], Michail I. Gladyshev[1,2]

1 Institute of Biophysics of Federal Research Center "Krasnoyarsk Science Center" of Siberian Branch of Russian Academy of Sciences, 50/50 Akademgorodok, Krasnoyarsk, 660036, Russia,

2 Siberian Federal University, 79 Svobodny avenue, Krasnoyarsk, 660041, Russia,

3 Department of Ecohydrology, Leibniz-institute of Freshwater Ecology and Inland Fisheries, Müggelseedamm 310, Berlin, 12587, Germany

4 Practical Center of the National Academy of Sciences of Belarus for Bioresources, 27 Akademicheskaya Street, 220072, Minsk, Belarus

5 Department of Biosciences, Swansea University, SA2 8PP, U.K.

* corresponding author e-mail: dubovskaya@ibp.krasn.ru

Running head: Zooplankton non-predatory mortality

Keywords: zooplankton, *Arctodiaptomus salinus*, non-predatory mortality, sediment trap, carcasses, stratified lake

Abstract

Zooplankton populations can at times suffer mass mortality due to non-predatory mortality (NPM) factors, and the resulting carcasses can be captured by sediment traps to estimate NPM rate. This approach assumes sinking to be the primary process in removing carcasses, but in reality carcasses can also be removed by ingestion, turbulent mixing and microbial degradation in the water column. We presented mathematical formulations to calculate NPM from sediment trap data by accounting for carcass removal by processes in addition to sinking, and demonstrated their application in a study in Lake Shira, Russia. Carcass abundance of the major calanoid copepod *Arctodiaptomus salinus* decreased with depth, indicating the effect of carcass removal from the water column. The estimated NPM values (0.0003–0.103 d^{-1}) were comparable to previously reported physiological death rates. We further used independent data to partition carcass removal due to detritivory, turbulent mixing and microbial degradation. Estimated ingestion by the amphipod *Gammarus lacustris* could account for the disappearance of copepod carcasses above the traps. Wind-driven turbulence could also extend the carcass exposure time to microbial degradation. Collectively, these water column processes would facilitate the remineralization of carcasses in the water column, and diminish the carcass carbon flux to the benthos.

Introduction

Zooplankton population dynamics is determined by two fundamental processes: Birth and death. In contrast to birth rate, estimation of *in situ* zooplankton mortality is logistically challenging (Dubovskaya, 2009; Tang and Elliott, 2013; Kimmerer, 2015). Apart from predation, zooplankton can suffer non-predatory mortality (NPM) caused by, e.g., senescence, environmental stresses, food limitation, diseases and parasitism (Tang et al., 2014), and leave behind carcasses. The importance of NPM in constraining zooplankton population growth has been demonstrated theoretically (Gentleman and Head, 2017) and empirically (Elliott and Tang, 2011). It can account for on average 25-33% of the total mortality among epi-pelagic marine copepods (Hirst and Kiørboe, 2002; Elliott and Tang, 2011); in some cases, NPM is the main cause of zooplankton population collapse (e.g. Gries and Gude, 1999; Dubovskaya et al., 2003; Wagner et al., 2004).

Sediment traps are widely used to collect sinking matter for characterization and to quantify sinking fluxes (Buesseler et al., 2007), and appearance of zooplankton carcasses (distinguishable from swimmers) in sediment traps indicates the role of sinking in removing zooplankton carcasses from the water column (Frangoulis et al., 2011; Dubovskaya et al., 2015). Several sediment trap studies have highlighted the contribution of zooplankton carcasses to the carbon sinking flux (Sampei et al., 2009, 2012; Ivory et al., 2014); sediment trap data also have been used to estimate carcass sinking rates and NPM (Dubovskaya et al., 2015).

In addition to sinking, zooplankton carcasses can be removed by a multitude of water column processes such as microbial decomposition, detritivory and turbulent mixing before the carcasses reach the traps (Dubovskaya, 2008; Elliott et al., 2010; Kirillin et al., 2012). Indeed, a decrease in carcass abundance with depth has been reported (e.g., Bickel et al., 2008). Therefore, proper calculation of NPM requires knowledge of both the mean carcass abundance in the water column above the sediment trap ($\bar{y}$) and carcass abundance at sediment trap depth (y^*). By comparing $\bar{y}$ and y^*, we can also gain insights into the relative importance of sinking vs. other removal processes in controlling the fate of zooplankton carcasses. In the simplest terms, we can consider two scenarios: (i) $\bar{y} \leq y^*$ suggests sinking dominates over other processes in removing carcasses from the water column; (ii) $\bar{y} > y^*$ suggests other processes are also important in removing carcasses (see Methods section for details).

Here we use Lake Shira, a fishless brackish meromictic lake in Russia, as a model system to study in situ NPM and carcass dynamics of the dominant species *Arctodiaptomus salinus* (Copepoda: Calanoida). The objectives were to estimate NPM from sediment trap data and investigate the relative importance of sinking vs. other removal processes—encapsulated by the removal coefficient D—in controlling carcass dynamics in the water column. We further attempted to partition D by independently estimating carcass removal due to microbial degradation, turbulent resuspension, and detritivory by the dominant invertebrate predators.

Methods

Non-predatory mortality estimation

Table I explains the symbols used in equations and text. *In situ* NPM estimations are based on the equation of vertical transport in time (t) and depth (z) coordinates with a source term in the following form:

$$\frac{\partial y(z,t)}{\partial t}=m(z,t)N(z,t)-\frac{\partial F(z,t)}{\partial z}, \qquad (1)$$

where t is time, z is depth, m (d^{-1}) is the specific non-predatory mortality, F is the vertical flux of carcasses, N and y are abundances of live individuals and carcasses (ind m^{-3}), respectively. Integration of Eq. (1) over the layer $0 < z < h$ above the sediment trap, under the assumption of zero flux of carcasses across the air-water boundary $F(0) = 0$, yields:

$$\frac{d\overline{y}(t)}{dt}+\frac{F^*(t)}{h}=\overline{m(z,t)N(z,t)}, \qquad (2)$$

where the overbar means averaging over the water column $0 < z < h$; the vertical flux F^* of carcasses at the trap exposure depth h (ind m^{-2} d^{-1}) is directly measured as

$$F^* \equiv v^* y^* = \frac{Y}{S}, \qquad (3)$$

and

$$v^* = Y/(Sy^*). \qquad (4)$$

Here, Y is number of carcasses accumulated in a sediment trap per day (ind d^{-1}), S is the input area of the trap (m^2), v^* (m d^{-1}) and y^* (ind m^{-3}) are the sinking velocity of carcasses and the concentration of the carcasses at trap exposure depth (outside the trap), respectively. In what follows the arguments of functions dependent on time and depth are not indicated, unless they are indispensable (e. g. y in Eq. 1 is clearly a function of depth and time, but its spatial average $\overline{y}$ is a function of z only). The final expression of the depth-averaged specific non-predatory mortality m becomes

$$m=\frac{1}{\overline{N}}\left(\frac{d\overline{y}}{dt}+Gy^*\right), \qquad (5)$$

subject to subsequent integration with respect to time based on discrete series of measurements on y^* and v^* (hereinafter, we omit the overbar over m for simplicity). Here,

$$G=\frac{v^*}{h} \qquad (6)$$

is the specific rate of elimination of carcasses from the water column via sinking. In order to explore the application of Eq. 1 and Eq. 5 to estimate NPM, we consider a simple case of depth-constant sinking velocity v. Then, Eq. 1 becomes

$$\frac{\partial y}{\partial t} = mN - v\frac{\partial y}{\partial z}. \tag{7}$$

Assuming further that live zooplankton are homogeneously distributed throughout the water column (N=constant), and the situation is close to steady state ($\partial y/\partial t \approx 0$), Eq. 1 is solved as

$$y = (mN/v^*)z + y_{0,} \tag{8}$$

i.e. abundance of carcasses y should increase linearly with depth unless they are removed before reaching the trap. This equation however does not take into account various processes other than sinking, such as turbulence, degradation and detritivory, in removing carcasses from the water column. The combined effect of these processes can be represented by adding a first-order removal rate with a coefficient D to Eq. 1:

$$\frac{\partial y}{\partial t} = mN - v\frac{\partial y}{\partial z} - Dy. \tag{9}$$

In contrast to Eq. 8, solution to Eq. 9 yields exponentially decaying y with depth. To explore its effect on m, we further reduce the number of independent variables by assuming the instantaneous carcass abundance be proportional to the abundance of live zooplankton, $y = \delta N$. The analytical solution to Eq. 9 under the same assumptions N = constant and $\partial y/\partial t \approx 0$ is

$$y(z) = y_0 \exp\left(\frac{m - D\delta}{\delta v} z\right), \tag{10}$$

and the solution with respect to m, analogous to Eq. 5, can be written as

$$m = \frac{1}{\bar{N}}\frac{d\bar{y}}{dt} + \frac{1}{\bar{N}}\left(D\bar{y} + Gy^*\right). \tag{11}$$

Thus, the specific NPM m_{trap} as calculated from sediment trap data by Eq. 5 is reduced by relative loss rate, as compared with the real mortality *in situ*:

$$m_{trap} = m - D\frac{\bar{y}}{\bar{N}}. \tag{12}$$

At high removal rate D, carcass abundance at trap depth (y^*) approaches zero, and estimations of mortality from Eq. 5 become unreliable. Its alternative, Eq. 11 requires empirical measurement of D by extensive sampling and analysis of the plankton communities, which is logistically challenging to do. A practical solution is by adopting the integral sample of carcasses abundance over the entire water column as an approximation of their abundance at the trap deployment depth, i.e. $\bar{y} \approx y^*$, which turns Eq. 5 to:

$$m = \frac{1}{\bar{N}}\left(\frac{d\bar{y}}{dt} + G\bar{y}\right). \qquad (13)$$

This formulation was used for NPM estimations by Gladyshev and Gubanov (1996) (see also Gladyshev et al., 2003 for details).

By comparing Eq. 13 and Eq. 5; i.e. replacing y^* with $\bar{y}$, we can estimate the variance in m caused by elimination of carcasses above the trap depth. For example, introducing $\gamma = (D–m/\delta)/v$, one can show that $\bar{y}/y^* \rightarrow 1$ at $\gamma h \rightarrow 0$, and $\bar{y}/y^* \rightarrow \infty$ at $\gamma h \rightarrow \infty$, where h, as before, is the depth of the trap. Hence, Eqs. 5 and 13 are interchangeable if the traps are positioned close to the depth of the maximum abundance of zooplankton where carcasses are originated (Dubovskaya et al., 2015), and the error becomes higher with deeper deployment of traps. An intermediate case $\gamma h \approx 1$ yields $\bar{y}/y^*$ $\approx (e - 1) \approx 1.71$, i.e. Eq. 13 would in typical configurations slightly overestimate the mortality rate, but the overestimation is within the range of method accuracy. Eq. 13 becomes equivalent to Eq. 11

$$\text{if } D = G\left(1 - \frac{y^*}{y}\right). \qquad (14)$$

Hence, *in situ* mortality rates as produced by Eq.13 imply a depth- and time-constant elimination of carcasses at the rate given by Eq. 14. At small y^*, Eq. 14 suggests that the elimination of carcasses above the trap is nearly equal in magnitude to the removal of carcasses due to sinking:

$$D \approx G. \qquad (15)$$

For estimation of the NPM from discrete field sampling, a finite difference equivalent of Eq. 13 is used:

$$m_i = \frac{\Delta\bar{y}}{\Delta t \cdot \bar{N}_i} + G_i \cdot \frac{\bar{y}_i}{\bar{N}_i} \qquad (16)$$

Where m_i (d^{-1}) is the specific NPM at the time t_i (day), $\Delta t_i = t_{i+1} - t_i$, is the period between two sampling events i, $\bar{y}_i$ is the mean abundance of carcasses (ind.·m^{-3}) at t_i in the water column above the trap, $\Delta\bar{y} = \bar{y}_{i+1} - \bar{y}_i$, $\bar{N}_i$ is abundance of live individuals (ind.·m^{-3}) in the water column above the trap. Eq. 5 becomes:

$$m_i = \frac{\Delta\bar{y}}{\Delta t \cdot \bar{N}_i} + G_i \cdot \frac{y_i^*}{\bar{N}_i} \qquad (17).$$

The difference between Eq.16 and Eq. 17 is in using $\bar{y}$ vs. y^* in the last term. In the following we applied both Eq. 16 and Eq. 17 to estimate zooplankton NPM in Lake Shira, and to evaluate the relative importance of D vs. G.

Study site

Lake Shira (54.499°N, 90.204° E), situated in the steppe area of Khakassia Republic at 354 m above sea level, has been intensively studied for the last 2 decades (Zotina et al., 1999; Yemelyanova et al., 2002; Rogozin et al., 2010, 2016; see also special issues of Aquatic ecology 2002, 36 (2) and 2010, 44 (3)). The lake area is 35.9 km^2, the maximum depth is 24 m. The depth of the upper boundary of the anoxic monimolimnion with hydrogen sulfide varies seasonally and annually (Rogozin et al., 2010, 2016), and it was 20 m in the present study. The relative concentrations of the major ions are sulfate > chloride > bicarbonate, and sodium > magnesium. In recent years, the water level of the lake has increased, and salinity (as ash content) has decreased to below 14-15 g l^{-1} in the epilimnion and 18-19 g l^{-1} in deeper waters (Rogozin et al., 2010). Zooplankton in the pelagic and open littoral zones are dominated year-round by *Arctodiaptomus salinus* (Copepoda, Calanoida), with the addition of *Brachionus plicatilis* and *Hexarthra spp.* (Rotifera) (Zotina et al., 1999; Zadereev and Tolomeyev, 2007). The major predator in this fishless lake is the amphipod *Gammarus lacustris* in the littoral and the pelagic zones (Tolomeyev et al., 2006; Zadereev et al., 2010).

0 Our study was conducted on 18-30 June, 2015, at a deep point (water depth 20 m) of the lake, where sediment traps were deployed in the upper part of the hypolimnion. The related hydro-physical recordings were made at ca. 250 m away from the traps. The temperature profile was measured by a thermistor chain consisted of a common logger and 30 digital temperature sensors DS18b20 (Maxim Integrated Products, resolution 0.1°C, absolute accuracy 0.5°C) with a spacing of 0.5 m for depths 3.5 to 13.5 m, and of 1-1.5 m for the other depths. The scanning interval was 30 s. An upward-looking 600 kHz acoustic Doppler current profiler (ADCP, manufactured by Teledyne RDI-Instruments, USA) was deployed at 16 m. The ADCP scanned the water column on 25-30 June in 0.5 m bins at the sampling intervals of 2.66 s. The velocity profiles were internally averaged over 120 s. On 13 and 29 June, profiles of temperature and conductivity were taken with YSI-6600 V2 sonde (YSI Inc., USA). Wind speed and direction were measured by a land-based Vantage Pro 2 weather station (Davis Instruments, USA) located ~0.5 km from the lake at averaged intervals of 15 min.

Sediment traps and video recording

Three sediment traps were deployed close to each other at 14 ±1 m for three consecutive days from 18 to 21 June, and for 7 days from 24 to 30 June. The trap exposure time was 24 h, except on 24 June when the exposure time was 2 d (24-26 June) due to a storm on 25 June. Each trap consisted of a pair of cylindrical collectors (Hákanson, 1984). Each collector had the internal diameter of 0.103 m and the internal height of 0.7 m, and the height-to-diameter ratio of 6.8 satisfied the requirement to prevent resuspension (Hákanson et al., 1989). Before deploying, the cylinders were filled with water from 14 m depth pre-screened through an 80-µm mesh. Each trap was moored to an anchor and a submerged buoy, and marked by a surface float (Fig. 1). Upon trap retrieval, zooplankton samples from the paired collectors of each trap were pooled, concentrated on an 80-µm mesh and counted for carcasses (Y in Eqs. 3 and 4).

To check whether *Gammarus lacustris* could actively penetrate the traps, and whether some resuspension of sedimented material occurred during the deployment, one trap collector was equipped with a video-recorder and a light source (Fig. 1). The digital video recorder Prestige DVR-022 (China) in a waterproof housing was externally mounted to the bottom glass window of the cylinder and recorded in upward direction (640×480, 30 fps). The lower part of the cylinder was illuminated by a waterproof LED strip. The light intensity was low enough not to attract 'swimmers', but sufficient for video recording. Power for the video-recorder and LEDs was provided by a waterproof 12 V10 Ah battery case attached to the anchor (Fig. 1). Video data were processed using the ImageJ v.1.46 software. The video was converted to a stack of images. Each image (frame) was subsequently filtered to remove noise and background roughness, so that moving objects were clearly seen. The number of animals per image was automatically registered by the built-in particle analyzer of ImageJ. Five-hour long video recordings during the night and the day were taken on 21 and 26 June, respectively. The field of view was about 100 ml where copepods were easily recognizable; gammarids, if present, could be detected at a longer distance.

Water column zooplankton sampling

Zooplankton were collected near the traps daily at around 10-11 a.m. with an open-close Juday net (80 µm mesh and mouth dia. 20 cm) from 15 to 12 m depth to obtain carcass abundance at trap depth (y^*), and from 12 m to surface to obtain depth-averaged live and dead abundances above the trap, which were used to calculate weighted means of N_i and y_i for 0-15 m layer (see *Mortality calculations*). Additional stratified net tows were done to obtain vertical distributions of live and dead *A. salinus* at 3-0, 6-3, 9-6, 12-9 and 15-12 m on 21 July (7-8 a.m.), 24 July (9-10 a.m. and 11-12 p.m.) and 28-29 July (11 a.m. and 12 p.m.).

Staining and counting of zooplankton

To distinguish between live and dead zooplankton, samples from the net and sediment traps were stained within an hour after collection with water-soluble aniline blue (Dubovskaya, 2008; Bickel et al., 2009) using a staining device (Gladyshev et al., 2003), and fixed in 10% formalin. Before counting, each sample was acidified according to Bickel et al. (Bickel et al., 2009). In the samples, only the most abundant species, *Arctodiaptomus salinus,* was counted under a microscope for live (unstained) and dead (stained blue) males, females, copepodites V (C5), copepodites I-IV

(C1-4) and nauplii. Fragmented carcasses and exuviae were not counted. *Gammarus lacustris,* as potential ‘swimmer’ and consumer of *A. salinus,* was also counted.

In situ carcass sinking velocity

Daily *in situ* sinking velocities of carcasses (v^*) of each developmental stage were calculated according to Eq. 4. The input area S was 0.0167 m^2 per trap. y^*_{av} was calculated as the average of samples taken at the beginning and at the end of the daily trap exposure, or the average of the two samples plus an additional night sample (Table I).

Mortality calculations

Specific NPM (m) of *A. salinus* nauplii, C1-4, C5, males and females were calculated for layer 0–15 m using Eqs.16 and 17 for three periods, 19-21 June (Δt_1), 21-26 (Δt_2) and 24-29 June (Δt_3). Weighted means of abundance of these stages for 0-15 m ($\bar{N}_i$, $\bar{y}_i$ and $\bar{y}_{i+1}$ in Eqs 16, 17) were calculated for each day as [$N_{(0\text{-}12)}$ × 12m + $N_{(12\text{-}15)}$ × (15-12m)]/15m or [$N_{(0\text{-}3)}$+$N_{(3\text{-}6)}$+$N_{(6\text{-}9)}$+$N_{(9\text{-}12)}$+$N_{(12\text{-}15)}$]/5, where $N_{(0\text{-}12)}$, $N_{(12\text{-}15)}$, $N_{(0\text{-}3)}$, $N_{(3\text{-}6)}$, $N_{(6\text{-}9)}$, $N_{(9\text{-}12)}$ and $N_{(12\text{-}15)}$ are abundances in the corresponding layers 0-12 m, 12-15 m, 0-3 m, 3-6 m, 6-9 m and 9-12 m. The means for 24 and 29 June were taken as the average of the day-night data. The specific rate of elimination due to sinking (G) was calculated from Eq. 6 using the water column depth above the traps h = 14 m. Daily sinking velocity (v^*) was time-averaged for Δt_1, Δt_2 and Δt_3.

Steps were taken to minimize potential errors in estimating live and dead *A. salinus* abundances as described in Dubovskaya et al. (2015): (i) traps were exposed for 24±1 h (48 h for 24-26 June) to increase accuracy of Y; (ii) two to three replicate traps were exposed simultaneously to increase accuracy of Y by increasing the total value of S and to increase precision of Y; (iii) large volume plankton samples (94-376 L) were collected at trap depth and in the overlying water column to increase accuracy of y^*, $\bar{N}_i$ and $\bar{y}_i$; (iv) sampling at trap depth was done 2–3 times per day to increase precision of y^* and to integrate daily variations (patchiness) of y^*.

Estimation of stratification and turbulence

The background stratification and mixing conditions were estimated from the profiles of density ρ and the coefficient of the vertical turbulent exchange K_Z. Water density as a function of time and depth $\rho(z, t)$ was calculated from temperature and salinity following Millero et al. (Millero et al., 1980). The time- and depth-resolved temperatures were taken from the thermistor chain, the salinity profile was obtained by averaging the conductivity profiles of four CTD casts in the vicinity of the thermistor chain. Conductivity was transformed to salinity using the specific formula based on the ion composition of Lake Shira (Rogozin et al., 2010).

The coefficient of vertical turbulent exchange K_Z at depth z was estimated by integrating the vertical density transport from the lake bottom *H* to *z*:

$$\int_H^z \frac{\partial \rho}{\partial t} = \int_H^z \frac{\partial}{\partial z} K_Z \frac{\partial \rho}{\partial z} \tag{18}$$

or

$$\int_H^z \frac{\partial \rho}{\partial t} = \left(K_Z \frac{\partial \rho}{\partial z} \right)_z - \left(K_Z \frac{\partial \rho}{\partial z} \right)_H . \tag{19}$$

Neglecting the vertical density gradient at the lake bottom, the final expression for K_Z is

$$K_Z = -\frac{\int_H^z \frac{\partial \rho}{\partial t}}{\left(\frac{\partial \rho}{\partial z} \right)_z} \tag{20}$$

which is subsequently solved numerically using finite differences for differentiation and trapeze method for integration.

Statistical analysis

Standard deviation (SD), coefficient of variation (CV), standard error (SE) were calculated conventionally using the STATISTICA software, 9.0 (StatSoft Inc., Tulsa, OK, U.S.A). Relative error (%) was calculated as RE = (SE/mean value) × 100.

Results

Environmental conditions, thermal stratification and turbulence

The daily mean wind speed varied from 1.8 to 4.6 m s^{-1}, and the current speed at the sediment trap depth of 14 m was ≤ 4.6 cm s^{-1} (Fig. 2A). Daily mean water temperature varied slightly from 18.6 to 20.6°C in the epilimnion (0-6 m), increased from 7.7°C on 19th June to 10.7°C on 29th June in the thermocline (6-12 m), and increased slightly from 1.4°C on 18-21th June to 1.8°C on 30th June in the upper oxic hypolimnion (12-15 m). Temperature at the trap depth varied during the study from 0.6 to 2.8°C with the mean of ca. 2°C (Fig. 2 B,C).

Overall, the water column consisted of a shallow epilimnion exposed to wind mixing, a strong thermocline starting at ~6 m depth and a halocline starting at ~9 m depth. The resulting pycnocline occupied the layer of 8-15 m depth with a density gradient of ~5 kg m^{-3} across (Fig. 2C). The lower part of the pycnocline, between ~12 m and 15 m, was occupied by a cold oxic hypolimnion with an anoxic monimolimnion beneath. High turbulent mixing intensity at the lake surface with K_Z up to

10^{-1} m^2 s^{-3} (Fig. 2D) was apparently produced by wind, in particularly during the storm events on 21-22 June and 24-26 June (Fig. 2A). K_Z quickly decreased with depth to < 10^{-5} m^2 s^{-3} close to the lake bottom, which can be treated as non-turbulent background value when taking into account the accuracy of the method. A small local maximum of mixing intensity between 14 and 16 m depth (Fig. 2D) was likely the result of internal wave breaking, as indicated by the isotherm oscillations (Fig. 2B).

Vertical distribution of live and dead Arctodiaptomus salinus

Live nauplii and small copepodites (C1-4) were abundant in the epilimnion (0-6 m) with near surface maxima (0-3 m, Fig. 3). Live males and females occupied the epilimnion and the upper metalimnion (0-9 m), with their maximal abundances in the 0-3 m layer (Fig. 3). Live late copepodites (C5) congregated in the metalimnion (6-12 m) (Fig. 3). Copepodites C5 contained many visible fat droplets in their bodies. Abundances of C5 and adults were substantially lower than that of nauplii and copepodites C1-4, which dominated the population (Fig. 3). The nighttime vertical distribution of all stages was similar to that in the daytime (Fig. 3).

Carcass abundances of all stages were low (Fig. 3). Vertical distribution of carcasses generally followed that of live animals. However, in many cases, the carcass abundance maxima were located below the live copepod abundance maxima. The abundances of both live and dead individuals of all stages, except C5, were lowest in the trap layer (12-15 m) (Fig. 3).

Trap and water column samples

The number of *A. salinus* carcasses accumulated in the traps per day (Y) varied considerably during the study period (Table II). Kolmogorov–Smirnov test showed a normal data distribution for each stage: $D_{K\text{-}S}$ varied from 0.21 ($p = 0.29$) for females to 0.27 ($p = 0.08$) for C5. Relative errors in Y estimation varied from low (0–14% for different stages; Table II) to high under low carcass abundance (100% for nauplii, 43% for C1-4 and for males, 67% for C5 and 60% for females; Table II). Errors averaged for the whole period for the different stages were rather low, 22-47% (Table II). Relative errors of estimation of carcass abundance at trap depth (y^*_{av}) also varied widely, with average values of 22-38% (Table II). y^*_{av} values showed normal distribution: $D_{K\text{-}S}$ ranged from 0.17 ($p = 1.0$) for C5 to 0.25 ($p = 0.63$) for C1-4.

At the trap depth (12-15 m), no individuals of *Gammarus lacustris* were found (Table III). This species occupied the overlying water column 0-12 m, with maximal abundance at 0-3 and 3-6 m (Table III). The maximal concentration observed was 29 ind m^{-3}, which occurred the morning after the storm on 25 June. One swimmer of *G. lacustris* per trap was found sporadically, on a total of only 4 occasions (Table III). The gut of the first swimmer (18-19 June) was empty, the guts of the others, as well as gammarids from the net samples, contained *A. salinus* remains (of males, females, copepodites, eggs), but it could not be determined whether live or dead *A. salinus* individuals were ingested.

Video recordings confirmed very stable conditions of the water column. Even when changing currents pushed the traps around over the line, no resuspension was seen. During the day, the number of *A. salinus* in the field of view did not change (Fig. 4). Slight increase in number could be seen at night before sunrise, but it returned to previous level after two hours (Fig. 4). These changes obviously did not affect the calculations of sinking rates of *A. salinus* carcasses. No *G. lacustris* was seen in any of the video recording, confirming that the amphipod rarely, if ever, entered the traps (Table III).

Carcass sinking velocity

In situ sinking velocity of *A. salinus* carcasses varied among traps and days (Table IV). Males and females, which were larger than the other stages, had the highest v^* values, averaging 8.3 and 8.5 m d^{-1}, respectively (Table IV). Interestingly, copepodites C5, which were similar to adults in size but contained many fat droplets indicative of diapause, had the lowest average sinking velocity at 2.0 m d^{-1}.

Mortality estimations

Mean abundances of live and dead individuals of *A. salinus* of each developmental stage in the layers 0-15 m ($\overline{N}_i$, $\overline{y_i}$ and $\overline{y_{i+1}}$ in Eqs 16, 17) and 12-15 m (y_i* in Eq. 17) for calculation of NPM are presented in Table V. Each $\overline{y_i}$ value was higher than the corresponding y_i* value with the two exceptions for C5. Consequently, ($\overline{y_i} - y_i$*) values were rather high and (y_i*/$\overline{y_i}$) quite low, with two exceptions (Table V). The coefficient G, which represents carcass removal via sinking, ranged from 0.067 to 0.869 d^{-1}, with an average of 0.402 d^{-1}. The coefficient D, which represents carcass removal by other processes above trap depth, ranged from 0.021 to 0.823 d^{-1}, with an average of 0.361 d^{-1} (Table VI). The mortality rates (m) calculated with y_i* were very low, varying from -0.009 to 0.034 d^{-1} (Table VI). Conversely, m calculated with $\overline{y_i}$ were higher, at 0.0003-0.103 d^{-1} with one negative value, -0.002 (Table VI). Evidently, the negative values were within range of precision of the method, and therefore should be interpreted as ca. zero mortality. The mortality of all stages was highest at the beginning of the study, between 19 and 21 June (Table VI). This period coincided with the occurrence of maximal percentages of dead individuals of all stages (5-10 % in 0-15 m, 26-83 % in 12-15 m), and was followed by a noticeable decrease in the abundances of live individuals, most noticeably in nauplii, females and males ($\overline{N}_i$ on 21 and 24 June; Table V). Minimal mortality of all stages was in the last five-day period, 24-29 June (Table VI). Among all stages, females had the highest mortality (0.103-0.023 d^{-1}) and copepodites C5 the lowest (0.008-0.0003 d^{-1}) (Table VI).

Discussion

Consideration of trap performance

Appropriate choice of sediment trap design and dimensions is crucial for avoiding under-or over-trapping (Buesseler et al., 2007). According to Lau (1979), for a cylindrical trap with an aspect ratio of 6.8, resuspension starts when the trap Reynolds number exceeds 15000. Given our trap dimensions and *in situ* kinematic viscosity of 0.017 cm^2 s^{-1}, such Reynolds number is obtained only at a flow velocity of 24.7 cm s^{-1}, which is much higher than the observed flow velocity at the trap depth (3-4.6 cm s^{-1}). Thus, resuspension from our traps was unlikely. Our video recording also showed no physical disturbance near the trap bottom. Another possible source of error is trap tilt resulting in over-trapping (Gardner, 1985). Our trap design according to Håkanson (1984) kept the cylinders vertically stable irrespective of cable inclination; cable motions and vibrations were further minimized by a subsurface tension buoy (Bloesch and Burns, 1980). Hence, error due to trap tilt would be negligible (Gardner, 1985). Overall, the relative errors of our trap data (22-43%, Table II) indicate good trap precision (Stanley et al., 2004; Buesseler et al., 2007).

According to our data, there were no marked daily changes in the vertical distribution of dead and live *A. salinus* (Fig. 3). Similarly, Zadereev and Tolomeyev (2007) did not observe any large-scale diel vertical migrations (DVM) of *A. salinus* in the fishless Lake Shira. Therefore, our sampling and calculations were not affected by DVM.

Comparison of $\bar{y}$ and y^*

The population of *A. salinus* was concentrated in the upper 0-9 m, where the largest number of carcasses was found (Fig. 3). The decrease in carcass abundance with depth (Fig. 3) is consistent with the observations of Bickel et al. (2009), and suggests that carcass dynamics was affected by processes other than sinking. Both $\bar{y}$ and y^* were estimated with accuracy and precision of the same order of magnitude as those of other field studies (e.g. Dubovskaya et al., 2003). Error (*Er*) of abundance estimation (*A*) by our net sampling method can be calculated as $Er = 2.01A^{0.78}$ (Gladyshev, 1985; Dubovskaya, 1987). This *Er* includes micro-horizontal variability (zooplankton patchiness). For data of $\bar{N}_i$, $\bar{y}$ and y^* (Table V), *Er* was within a range of 20-109%. *Er* of y^*_{av} in Table II (for sinking velocity calculation) varied within 0-81 %, comparable to that for *Bosmina* in Lake Stechlin (1-66 %; Dubovskaya et al., 2015). Although y^* and Y were more variable in a few cases than those reported by Dubovskaya et al. (2015), sampling replications and rather large volumes of zooplankton samples (≥ 94 L) gave a reasonably accurate estimation of $\bar{y}$ and y^*.

Except for two occasions, y^* was in all cases lower than $\bar{y}$, giving low averaged $y^*/\bar{y}$ values of 0.13-0.19 for all stages except C5 (0.77; Table V). This observation has important ramifications for understanding NPM and carcass dynamics in the lake. Given $\bar{y}>y^*$, it means that many carcasses were removed from the water column before they reached the traps. Under such a condition, the choice of proper formulations is crucial for NPM calculation. When applying Eq. 17 to our data, NPM was -0.009-0.034 d^{-1}; while using Eq. 16 increased NPM estimation to -0.002-0.103 d^{-1} (as explained above, the negative values should be interpreted as zero mortality within the range of precision of the method). The latter values are more realistic, since they follow from the assumption of non-negligible *D*, which is also supported by $\bar{y}>y^*$ in our observations (see Introduction and Methods). Hence, application of Eq. 17 to sediment trap data would underestimate NPM. Even a small difference in NPM, when propagating through time, could lead to vastly different population growth projections (Elliott and Tang, 2011).

Carcasses in the water column can be removed by e.g. detritivory or microbial degradation. Turbulent mixing can increase the retention time of carcasses in the epilimnion and decrease the ratio $y^*/\bar{y}$. The coefficient *D* in our calculations encapsulates the combined effect of these and other processes, but it does not distinguish their relative importance. Nevertheless, below we use independently collected data to examine the roles of these processes in removing zooplankton carcasses above the trap depth.

Possible ingestion of carcasses by Gammarus

The amphipod *Gammarus lacustris* was the main predator in the fishless Lake Shira. Consistent with the data by Zadereev et al. (Zadereev et al.,2010) and Tolomeyev et al. (Tolomeyev et al., 2006), *G. lacustris* occupied the 0-12 m layer, but not below (Table III). Therefore, *G. lacustris* would not affect *A. salinus* carcass abundance at the trap depth. Rare appearance of *G. lacustris* inside the traps also suggests that this predator had no effect on carcass abundance in the traps or calculation of carcass sinking velocity from trap data.

Previous studies in Lake Shira have shown *G. lacustris* as the top predator of live and dead individuals of *A. salinus* and Rotifera in the epi-and meta-limnion (Yemelyanova et al., 2002; Gubanov, 2009). We found *A. salinus* remains in the guts of *G. lacustris* from the net and trap samples. Although we could not determine the original vital state of the ingested individuals, our observations at least indicate that the amphipod could potentially ingest *A. salinus* carcasses above the trap depth and contribute to the removal coefficient *D*.

The potential loss of carcasses due to ingestion by *G. lacustris* could be estimated from the daily energy expenditure of the amphipod. An individual of *G. lacustris* with a body length of 10 mm weighs ca. 11.60 mg (Yemelyanova et al., 2002) and has a respiration rate of 4.2 μl O_2 ind^{-1} h^{-1}

at the epilimnic mean temperature of 20°C (Sushchenja, 1972). Its daily energy expenditure can be estimated as $R = (0.0042 \times 24 \times 4.86)/0.9 = 0.544$ mg ind^{-1}day^{-1}, where 4.86 cal ml^{-1} O_2 is oxycaloric coefficient and 0.9 cal mg^{-1} is caloric content of wet mass (Winberg, 1986). Assuming an assimilation efficiency of 0.8 (Winberg, 1986), the required prey consumption would be 0.680 mg ind^{-1} d^{-1}. Given a wet weight of 0.068 mg for adult *Arctodiaptomus* (Balushkina and Winberg, 1979), this is equivalent to a consumption of ~10 carcasses ind^{-1} d^{-1}. The mean abundance of *G. lacustris* in the 0-12 m layer was 17 (± 3) ind m^{-3}, which translates to a potential mean removal of 170 ind m^{-3} of adult *A. salinus* carcasses. This estimated value is comparable to the differences between $\bar{y}$ and y^* for female and male *A. salinus* carcasses (91-684 ind m^{-3}, Table V). Therefore, ingestion of carcasses by *G. lacustris* within 0-12 m could explain the loss of carcasses.

Turbulence effect and microbial decomposition

Among the nauplii, C1-4 and adults, the average carcass sinking velocity (v^*) increased in accordance with the increase in body size. An interesting exception was C5, which had the lowest carcass sinking velocity and it is likely due to the presence of fat droplets in its body (e.g. Stepanov and Svetlichnyyi, 1981). The presence of fat droplet may allow C5 (both live and dead) to achieve neutral buoyancy and congregate within 6-12 m as observed in our field sampling.

The *in situ* carcass sinking velocities of *A. salinus* (2.0-8.5 m d^{-1}) were in general much lower than those obtained by *in vitro* settling column method. For example, *in vitro* sinking velocity was 35.4 ± 15.6 m d^{-1} for *Acartia tonsa* C1-3 carcasses (Elliott et al., 2010), and 112.1 ± 20.3 m d^{-1} for *Eudiaptomus gracilis* adult carcasses (Kirillin et al., 2012). *In vitro* sinking velocity in the absence of any water motion and physical gradients should be regarded as “maximal” (Ploug et al., 2008), or “potential” sinking velocity (Grossart and Simon, 1998). In contrast, *in situ* sinking velocity calculated from Eq. 4 represents the average downward velocity of sinking and suspended particles (McDonnell et al., 2010; 2015). Carcasses may achieve positive buoyancy due to microbial decomposition and float upward (Elliott et al., 2010; Kirillin et al., 2012)—a phenomenon known as “anti-rain” of carcasses (Dubovskaya et al., 2015), and not be captured by the traps.

Wind-driven currents and turbulence may also decrease carcass sinking velocities, leading to a lower average v^* and a lower mortality rate that can be accounted for by carcass sinking. During our study, wind speed increased on 21-22 June and on 25-26 June, resulting in high-amplitude oscillations of the isotherms—indicator of intensified internal wave activity, and a ~3-fold increase in current speeds at the trap depth (Fig. 2A). Sinking of carcasses might be slowed down by shear turbulence during these periods. Indeed, on 24-26 June the traps yielded rather low values of carcass sinking velocity, especially trap No. 1 and 2 (Table IV). Minimal sinking velocity of male carcasses was obtained in this period (Table IV). This turbulence effect has been described by others: Dubovskaya et al. (Dubovskaya et al., 2003) showed that the sinking velocities of *Daphnia* and *Cyclops* carcasses (v, m d^{-1}) were negatively correlated with wind speed (u, m s^{-1}) as $v = 3.709u^{-0.984}$. Ivory et al. (Ivory et al., 2014) also found a negative relationship between carcass flux measured by traps (y, mg C m^{-2}day^{-1}) and mean current velocity at the trap depth (x, cm s^{-1}): $y = 105.9e^{-0.70x}$.

We suggest that turbulence increases the retention time of carcasses in the upper epilimnion, where they can be removed by ingestion and/or microbial degradation. Based on the measured mean sinking velocities (Table IV), carcasses of nauplii from the surface ($z = 0$ m) would reach the sediment trap at 14 m in 3.8 days, C1-4 carcasses in 2.7 days, and adult carcasses in 1.5 days. During this time, microbial degradation as a temperature-dependent process (Eq. 18 in Kirillin et al., 2012) would decrease the carcass excess density by respectively 0.0223, 0.0210 and 0.0188 g cm^{-3}. Assuming an initial carcass density of 1.045 g cm^{-3} (Elliott et al., 2010), microbial degradation would lower the carcass excess density by 50, 47 and 42%, respectively. Such a substantial loss of excess density would greatly increase carcass retention time and remineralization above the traps.

The estimates of turbulent mixing from the flux-gradient method (Fig. 2D) also suggest high mixing rates in the epilimnion, apparently driven by wind. The K_Z values in the upper mixed layer of Lake Shira are up to one order of magnitude higher (10^{-1} m^2 s^{-3}) than those measured previously in the similarly sized but more wind-sheltered Lake Stechlin (10^{-3}-10^{-2}m^2 s^{-3}, Kirillin et al., 2012). Interestingly, according to the random-walk model of turbulence (Kirillin et al., 2012), this increase of K_Z does not produce any significant increase in carcass retention in the epilimnion. Apparently, isotropic chaotic movements have little effect on carcass sinking. However, the circular water motions produced by surface waves, Langmuir circulations, or convective cells may capture relatively small particles (e.g. zooplankton carcasses) for a longer time and contribute to their mechanical destruction. A reliable quantification of these effects requires *in situ* observation of carcasses movement in surface waters.

The stratification in the brackish Lake Shira is appreciably stronger than in freshwater lakes. For example, the density gradient across the Lake Shira pycnocline was ~5 kg m^{-3}, compared to only ~2 kg m^{-3} in Lake Stechlin and Lake Arend (Kirillin et al., 2012). The strong stratification in Lake Shira could further slowdown carcass sinking and promote their degradation in the water column.

Reality check of non-predatory mortality estimates

The decrease in carcass abundance with depth indicates that a significant amount of carcasses was eliminated from the water column above the traps. However, the processes of carcass elimination are difficult to parameterize due to limited observational information, and the removal term remains poorly constrained. Only a rudimentary approach to this problem was attempted by Frangoulis et al. (Frangoulis et al., 2011), who attributed the decrease in carcass flux with increasing depth to decomposition of the sinking material. Hence, the reliability of the otherwise well-established and robust sedimentation trap method to estimate zooplankton NPM requires a more thorough evaluation.

Incorporation of removal processes in addition to sinking (Eqs. 9 and 16) produces conservative NPM estimates of 0.0003–0.103 d^{-1}, which are comparable to the non-predatory mortality rates for zooplankton reported in the literature (<0.01-0.15 d^{-1}; reviewed by Tang and Elliott, 2013). For example, the rich fat content observed in C5 was indicative of diapause, and the estimated m for C5 (0.0003-0.008 d^{-1}) was indeed close to the minimal physiological death rate of 0.001-0.05 day^{-1} (Shushkina et al., 2000; Dubovskaya, 2009). Two of the three m values for females (0.048-0.023) and males (0.049-0.020), on the other hand, were close to the upper limit of senescence death rate of 0.01-0.05 day^{-1} (Tang et al., 2014). The same range of NPM values was reported by Frangoulis et al. (Frangoulis et al., 2011) for copepods derived from “swimmer-excluding” sediment trap data. The minimal mortality of adult calanoid copepods in survival experiments was also within the range of 0.001-0.031 d^{-1} (Kiørboe et al., 2015).

Furthermore, the temporal variation of NPM values was consistent with *A. salinus* abundance data. For example, the relatively high mortality of all developmental stages (the population average 0.061 d^{-1}; Table VI) at the beginning of the study period (19-21 June) was followed by a decrease in the abundance of live nauplii, C1-4, males and females between 21 and 24 June (Table V). During the following intervals Δt_2 and Δt_3, the NPM value decreased initially to 0.022 d^{-1} on average and to 0.007 d^{-1}afterwards, and the concurrent variations in the abundance of all developmental stages were also low, suggesting that the population was close to equilibrium.

Conclusion

Notwithstanding the ignorance of zooplankton carcasses in conventional field sampling, it is now evident that zooplankton can suffer, at times significantly, non-predatory mortality and leave behind carcasses. Sediment trap method has been well developed and widely used for studying sinking fluxes. By using sediment traps to collect sinking zooplankton carcasses *in situ*, it is possible to derive NPM from the trap data, as well as to assess the contribution of zooplankton carcasses to organic carbon flux. Hence, sediment traps, when augmented by water column sampling, provide an effective means to investigate zooplankton non-predatory mortality and the fate of the carcasses. However, the sediment trap method assumes sinking as the major (sole) process removing carcasses. Accordingly, the accuracy of the method can be compromised when carcasses are removed by other processes in the water column before they reach the traps.

In this study, we began with a detailed mathematical analysis of the problem and derived formulations to account for carcass removal from the water column. We then used an empirical study in Lake Shira to compare and contrast the use of depth-integrated average carcass abundance ($\overline{y}$) and depth-specific carcass abundance (y^*) for calculating NPM of the dominant copepod *A. salinus*, and to examine the different water column processes for removing copepod carcasses. We showed that in Lake Shira where carcass abundance decreased with depth, it is essential to take into account removal of carcasses in addition to sinking when calculating NPM. To a first approximation, it can be done by adopting the mean abundance of carcasses in the water column above traps ($\overline{y}$) as a characteristic value for estimation of the NPM from the trap data. We also showed that ingestion by the amphipod *G. lacustris*, along with turbulent mixing and microbial degradation, could account for the estimated removal of carcasses above trap depth.

The observation that y^* was considerably smaller than $\overline{y}_i$ means that a good portion of the zooplankton carcasses was retained in the upper water layer, thereby contributing to epilimnic carbon and nutrient cycling, rather than to the benthic food web in Lake Shira.

Funding

This work was a part of the joint German-Russian Project “Mortality of Zooplankton in lake ecosystems and its potential contribution to carbon mineralization in pelagic zone” supported by the German Research Foundation [DFG Nr. GR-1540/29-1] and the Russian Foundation for Basic Research [RFBR No. 16-54-12048]. The work also was partly supported by Russian Federal Tasks of Fundamental Research [project No. 51.1.1] and by grant [NSh-9249.2016.5] from the President of the Russian Federation.

References

Balushkina, E. V. and Winberg, G. G. (1979) Relation between mass and body size of plankton animals. In Winberg, G. G. (ed), *General backgrounds for study of aquatic ecosystems*. Nauka, Leningrad, pp. 169–172. (in Russian)

Bickel, S. L., Tang, K. W. and Grossart, H.-P. (2009) Use of aniline blue to distinguish live and dead crustacean zooplankton composition in fresh waters. *Freshwater Biol.*, **54**, 971–981.

Bloesch, J. and Burns, N. M. (1980). A critical review of sediment trap technique. *Schweiz. Z. Hydrol.*, **42**, 15-55.

Buesseler, K. O., Antia, A. N., Chen, M., Fowler, S.W., Gardner, W.D., Gustafsson, O., Harada, K., Michaels, A. F., et al. (2007) An assessment of the use of sediment traps for estimating upper ocean particle fluxes. *J. Mar. Res.*, **65**, 345–416.

Dubovskaya, O. P. (1987) Formation of zooplankton of Sayano-Shushensk reservoir. PhD Thesis. Irkutsk State University. (in Russian)

Dubovskaya, O. P. (2008) Evaluation of abundance of dead crustacean zooplankton in a water body using staining of the samples by aniline blue technique: methodological aspects. *J. SibFU. Biol.*, **1**, 145-161. (in Russian)

Dubovskaya, O. P. (2009) Non-predatory mortality of the crustacean zooplankton, and its possible causes (a review). *Zh. Obshch. Biol.*, **70**, 168–192 (in Russian).

Dubovskaya, O. P., Gladyshev, M. I., Gubanov, V. G. and Makhutova,O. N. (2003) Study of non-consumptive mortality of Crustacean zooplankton in a Siberian reservoir using staining for live/dead sorting and sediment traps. *Hydrobiologia*, **504**, 223-227.

Dubovskaya, O. P., Tang, K. W., Gladyshev, M. I., Kirillin, G., Buseva, Z., Kasprzak, P., Tolomeev, A. P. and Grossart, H. -P. (2015) Estimating in situ zooplankton non-predation mortality in an oligo-mesotrophic lake from sediment trap data: caveats and reality check. PLoS ONE, **10**(7), e0131431 [doi:10.1371/journal.pone.0131431].

Elliott, D. T., Harris, C. K. and Tang, K. W. (2010) Dead in the water: the fate of copepod carcasses in the York River estuary, Virginia. *Limnol. Oceanogr.*, **55**, 1821–1834.

Elliott, D. T. and Tang, K. W. (2011) Influence of carcass abundance on estimates of mortality and assessment of population dynamics in *Acartia tonsa*. *Mar. Ecol. Prog. Ser.*, **427**, 1-12.

Frangoulis, C., Skliris, N., Lepoint, G., Elkalay, K., Goffart, A., Pinnegar, J. K. and Hecq, J.-H. (2011) Importance of copepod carcasses versus faecal pellets in the upper water column of an oligotrophic area. *Estuar. Coastal Shelf Sci.*, **92**, 456–463.

Gardner, W. D. (1985) The effect of tilt on sediment trap efficiency. *Deep-Sea Res.*, **32**, 349-361.

Gentleman, W. C. and Head, E. J. H. (2017) Considering non-predatory death in the estimation of copepod early life stage mortality and survivorship. *J. Plankton Res.*, **39**, 92–110.

Gladyshev, M. I. (1985) Assessment of the statistical significance of differences in zooplankton abundance on single samples. *Gidrobiol. Zh.*, **21**(5), 65–70. (In Russian).

Gladyshev, M. I., Dubovskaya, O. P., Gubanov, V. G. and Makhutova, O. N. (2003) Evaluation of non-predatory mortality of two *Daphnia* species in a Siberian reservoir. *J. Plankton Res.*, **25**, 999-1003.

Gladyshev, M. I. and Gubanov, V. G. (1996) Seasonal dynamics of specific mortality of *Bosmina longirostris* in forest pond determined on the basis of counting of dead individuals. *Dokl. Akademii Nauk*, **348**(1), 127-128.

Gries, T. and Güde, H. (1999) Estimates of the nonconsumptive mortality of mesozooplankton by measurement of sedimentation losses. *Limnol. Oceanogr.*, **44**, 459-465.

Grossart, H.-P. and Simon, M. (1998) Significance of limnetic organic aggregates (lake snow) for the sinking flux of particulate organic matter in a large lake. *Aquat. Microb. Ecol*., **15**, 115-125.

Gubanov, M. V. (2009) Interspecific interactions of dominant species of lake Shira biota in laboratory conditions. PhD Thesis. Krasnoyarsk, Sib.FU. (in Russian).

Hákanson, L. (1984) Suspension and calibration of a sediment trap. *Schweiz. Z. Hydrol*., **46**, 171-175.

Hákanson, L., Floderus, S. and Wallin, M. (1989) Sediment trap assemblages - a methodological description. *Hydrobiologia*, **176/177**, 481-490.

Hirst, A. G. and Kiørboe, T. (2002) Mortality of marine planktonic copepods: global rates and patterns. *Mar. Ecol. Prog. Ser*., **230**, 195-209.

Ivory, J. A., Tang, K. W. and Takahashi, K. (2014) Use of Neutral Red in short-term sediment traps to distinguish between zooplankton swimmers and carcasses. *Mar. Ecol. Prog. Ser*., **505**, 107–117.

Kiørboe, T., Ceballos, S. and Thygesen, U. H. (2015) Interrelations between senescence, life-history traits, and behavior in planktonic copepods. *Ecology*, **96**, 2225-2235.

Kimmerer, W.J. (2015) Mortality estimates of stage-structured populations must include uncertainty in stage duration and relative abundance. *J. Plankton Res*., **37**, 939–952.

Kirillin, G., Grossart, H.-P. and Tang, K. W. (2012) Modeling sinking rate of zooplankton carcasses: Effects of stratification and mixing. *Limnol. Oceanogr*., **57**, 881–894.

Lau,Y. L. (1979) Laboratory study of cylindrical sedimentation traps. *J. Fish Res. Bd Canada*, **36**, 1288–1291.

McDonnell, A. M. P. and Buesseler, K. O. (2010) Variability in the average sinking velocity of marine particles. *Limnol. Oceanogr*., **55**, 2085–2096.

McDonnell, A. M. P., Boyd, P. W. and Buesseler, K. O. (2015) Effects of sinking velocities and microbial respiration rates on the attenuation of particulate carbon fluxes through the mesopelagic zone. *Global Biogeochem. Cycles*, **29**, 175–193.

Millero, F. J., Chen, C. T., Bradshaw, A., and Schleicher, K. (1980) A new high pressure equation of state for seawater. *Deep-Sea Res. Part A*, **27**, 255–264.

Ploug, H., Iversen, M. H., Koski, M. and Buitenhuis, E. T. (2008) Production, oxygen respiration rates, and sinking velocity of copepod fecal pellets: Direct measurements of ballasting by opal and calcite. *Limnol. Oceanogr*., **53**, 469–476.

Rogozin, D. Y., Genova, S. N., Gulati, R. D. and Degermendzhy, A. G. (2010) Some generalizations based on stratification and vertical mixing in meromictic Lake Shira, Russia, in the period 2002–2009. *Aquat. Ecol*., **44**, 485–496.

Rogozin, D. Y., Zykov,V. V. and Tarnovskii, M. O. (2016) Dynamics of purple sulfur bacteria in a meromictic saline lake Shunet (Khakassia, Siberia) in 2007–2013. *Microbiology*, **85**, 93–101.

Sampei, M., Hattori, H., Forest, A., and Fortiera, L. (2009). Significant contribution of passively sinking copepods to downward export flux in Arctic waters. *Limnol. Oceanogr*., **54**, 1894–1900.

Sampei, M., Sasaki, H., Forest, A., and Fortier, L. (2012). A substantial export flux of particulate organic carbon linked to sinking dead copepods during winter 2007–2008 in the Amundsen Gulf (southeastern Beaufort Sea, Arctic Ocean). *Limnol. Oceanogr*., **57**, 90-96.

Stanley, R. H. R., Buesseler, K. O., Manganini, S. J., Steinbergb, D. K. and Valdes, J. R. (2004) A comparison of major and minor elemental fluxes collected in neutrally buoyant and surface-tethered sediment traps. *Deep-Sea Res. I*, **51**, 1387–1395.

Stepanov, V. N. and Svetlichnyyi, L. S. (1981) *Research of hydromechanical characteristics of plankton copepods*. Naukova Dumka, Kiev, pp. 128 (in Russian).

Shushkina, E. A., Vinogradov, M. E. and Lebedeva, L. P. (2000) Processes of detritus production and fluxes of organic matter from epipelagic zone in different oceanic regions. Oceanology, **40**, 183-191.

Sushchenja, L. M. (1972) *Respiration intensity of crustaceans*. Naukova dumka, Kiev. (in Russian)

Tang, K. W. and Elliott, D. T. (2013) Copepod carcasses: Occurrence, fate and ecological importance. In Seuront, L (ed.) *Copepods: Diversity, Habitat and Behaviour*. Nova Science Publishers.

Tang, K. W., Gladyshev, M. I., Dubovskaya, O. P., Kirillin, G. and Grossart, H.-P. (2014) Zooplankton carcasses and non-predatory mortality in freshwater and inland sea environments. *J. Plankton Res*., **36**, 597-612.

Tolomeyev, A. P., Zadereev, E. S. and Degermendzhy, A. G. (2006) Fine stratified distribution of *Gammarus lacustris* Sars (Crustacea: Amphipoda) in the pelagic zone of the meromictic lake Shira (Khakassia, Russia). *Dokl. Biochem. Biophys*., **411**, 346–348.

Wagner, A., Hulsmann, S., Dorner, H., Janssen, M., Kahl, U., Mehner, T. and Benndorf, J. (2004) Initiation of the midsummer decline of *Daphnia* as related to predation, non-consumptive mortality and recruitment: a balance. *Arch. Hydrobiol*., **160**, 1-23.

Winberg, G. G. (1986) Backgrounds of estimating of biotic balance. In Alimov, A.F. (ed.) *An investigation of relationship between food supply and fish productivity by example of Transbaikalia lakes*. Leningrad, Nauka, p. 188-193 (in Russian).

Yemelyanova, A. Y., Temerova, T. A. and Degermendzhy, A. G. (2002) Distribution of *Gammarus lacustris* Sars (Amphipoda, Gammaridae) in Lake Shira (Khakasia, Siberia) and laboratory study of its growth characteristics. *Aquat. Ecol*., **36**, 245–256.

Zadereev, Y. S. and Tolomeyev, A. P. (2007) The vertical distribution of zooplankton in brackish meromictic lake with deep-water chlorophyll maximum. *Hydrobiologia*, **576**, 69–82.

Zadereev, E. S., Tolomeyev, A. P., Drobotov, A. V., Emeliyanova, A. Y. and Gubanov, M. V. (2010) The vertical distribution and abundance of *Gammarus lacustris* in the pelagic zone of the meromictic lakes Shira and Shunet (Khakassia, Russia). *Aquat. Ecol.*, **44**, 531–539.

Zotina, T. A., Tolomeyev, A. P. and Degermendzhy, N. N. (1999) Lake Shira, a Siberian salt lake: ecosystem structure and function. 1. Major physico-chemical and biological features. International J. Salt Lake Res., **8**, 211–232.

Table I: Major symbols, definitions and their units used in equations and text

Symbol	Definition	Units
t	Time	d
z	Vertical coordinate	m
S	Input area of the trap	m^2
h	Depth of sediment trap exposure	m
Y	Accumulation rate of carcasses in a sediment trap	ind d^{-1}
v^*	Sinking velocity of carcasses at trap exposure depth h	m d^{-1}
y	Abundance of carcasses	ind m^{-3}
$\bar{y}$	Overbar means averaging over the water column $0 < z < h$	ind m^{-3}
$\bar{y}_i$	Index i refers to discrete values at time t_i in finite-difference approximations	ind m^{-3}
y^*	Asterisk refers to values at trap exposure depth h (outside the trap)	ind m^{-3}
y^*_{i}	Abundance of carcasses at trap exposure depth at time t_i	ind m^{-3}
y^*_{av}	Average carcass abundance of samples taken at the beginning and at the end of the daily trap exposure, or of the two samples plus an additional night sample	ind m^{-3}
	*The sub- and superscripts i, *, and overbar have the same meaning as above when applied to the following variables*	
F	Vertical flux of carcasses	ind m^{-2} d^{-1}
N	Abundance of live individuals	ind m^{-3}
G	Specific rate of elimination of carcasses from the water column $0 < z < h$ via sinking	d^{-1}
D	Carcass removal rate via degradation and detritivory in the water column $0 < z < h$	d^{-1}
m	Specific non-predatory mortality (NPM)	d^{-1}

Table II: Number of *Arctodiaptomus salinus* carcasses accumulated in sediment traps per day (Y, ind d^{-1}) and carcass abundances at trap depth, 12-15 m, average of 2-3 samples taken at the beginning and the end of daily trap exposure (y^*_{av}, ind m^{-3}) in Lake Shira (for calculation of v^*) in 2015.

Date in June	Carcasses in sedimenttrap, Y					Carcasses at trapdepth (12-15 m), y^*_{av}		
	Trap1	Trap2	Trap3	*CV* (%)	*RE* (%)	Abundance	*CV*(%)	*RE* (%)
Nauplii								
18-19	nd	5	15	70.7	50	127	nd	nd
19-20	20	14	20	19.25	11.1	167	33.9	24
20-21	41	20	23	40.6	23.4	210	1.7	1.2
24-26	0.5	0.5	1	43.3	25	49	12.9	7.4
26-27	6	1	nd	101	71.4	69	32.8	23.2
27-28	1	0	nd	141.4	100	154	63.4	44.8
28-29	1	0	1	86.6	50	85	140.7	81.2
Mean	-	-	-	-	47.2	116.9	-	36.2
C1-4								
18-19	nd	5	9	40.4	28.6	64	nd	nd
19-20	9	9	11	12	6.9	83	31.7	22.4
20-21	33	12	33	46.6	26.9	146	43.6	30.8
24-26	3	3	2.5	10.2	5.9	81	15.6	9
26-27	13	12	nd	5.7	4	154	73.5	51.9
27-28	10	4	nd	60.6	42.9	483	72.9	51.6
28-29	7	2	4	58.1	33.5	329	106.9	61.7
Mean	-	-	-	-	22.1	200.8	-	37.6
C5								
18-19	nd	1	2	47.1	33.3	21	nd	nd
19-20	7	2	4	58.1	33.5	88	107.5	76
20-21	17	4	1	116	67	152	2.3	1.7
24-26	1	0	1.5	91.7	52.9	134	50.7	29.3
26-27	1	4	nd	84.9	60	165	40.8	28.9
27-28	2	7	nd	78.6	55.6	128	11.6	8.2
28-29	1	1	1	0	0	81	72	41.6
Mean	-	-	-	-	42.5	107.5	-	27.4
Females								
18-19	nd	2	8	84.6	60	21	nd	nd
19-20	13	8	9	26.5	15.3	48	78.9	55.8
20-21	24	8	6	77.9	45	74	0	0
24-26	2	1	3	50	28.9	25	48.5	28
26-27	3	4	nd	20.2	14.3	37	19.1	13.5
27-28	2	5	nd	60.6	42.9	48	16.4	11.6
28-29	1	6	3	75.5	43.6	28	77.4	44.7
Mean	-	-	-	-	36.3	37.8	-	21.9
Males								
18-19	nd	5	5	0	0	21	nd	nd
19-20	14	8	7	39.2	22.6	56	88.4	62.5
20-21	20	8	11	48	27.7	72	37.3	26.4
24-26	2	0.5	2	57.7	33.3	25	48.5	28
26-27	2	3	nd	28.3	20	27	82.7	58.5
27-28	2	5	nd	60.6	42.9	64	47.9	33.9
28-29	7	8	5	22.9	13.2	42	100	58
Mean	-	-	-	-	26.8	43.6	-	38.2

Table III: Number of *Gammarus lacustris* (ind. sample^{-1}) in the water column at trap depth and inside the traps in Lake Shira in 2015; dash – no samples.

Date in June	Water column					Trap depth	In traps		
	0-3 m	3-6 m	6-9 m	9-12 m	0-12 m	12-15 m	1	2	3
18	-	-	-	-	7	0	-	-	-
19	-	-	-	-	4	0	0	0	1
20	-	-	-	-	-	0	0	1	0
21	2	1	2	0	-	0	1	1	0
24	0	1	0	1	-	0	-	-	-
24 night	1	1	0	0	-	0	-	-	-
26	-	-	-	-	11	0	0	0	0
27	-	-	-	-	8	0	0	0	0
28	-	-	-	-	5	0	0	0	0
29 night	4	4	1	0	-	0	-	-	-
29	1	4	1	1	-	0	0	0	0

Table IV: *In situ* sinking velocity (v^*, m d^{-1}) of *Arctodiaptomus salinus* carcasses calculated from Eq. 4 using data from Table 1 for Lake Shira.

Date in June	Trap No	Nauplii	C 1-4	C5	Females	Males
18-19	1	2.36	4.69	2.86	5.72	14.29
	2	7.09	8.44	5.72	22.87	14.29
19-20	1	7.19	6.55	4.80	16.43	15.01
	2	5.03	6.55	1.37	10.11	8.57
	3	7.19	8.00	2.74	11.37	7.50
20-21	1	11.75	13.57	6.74	19.47	16.67
	2	5.73	4.93	1.58	6.49	6.70
	3	6.59	13.57	0.40	4.87	9.17
24-26	1	0.61	2.21	0.45	4.80	4.80
	2	0.61	2.21	0	2.40	1.20
	3	1.22	1.85	0.67	7.20	4.80
26-27	1	5.22	5.07	0.36	4.87	4.53
	2	0.87	4.68	1.46	6.49	6.80
27-28	1	0.39	1.24	0.94	2.53	1.89
	2	0	0.50	3.30	6.32	4.73
28-29	1	0.71	1.28	0.74	2.12	9.93
	2	0	0.36	0.74	12.73	11.35
	3	0.71	0.73	0.74	6.36	7.10
Mean ± SE		3.51±0.82	4.81±0.97	1.98±0.47	8.51±1.40	8.30±1.07
For mortality calculation						
19-21		6.62±0.93	8.29±1.24	3.28±0.80	12.16±2.38	11.52±1.39
21-26		4.42±1.82	6.39±3.58	1.64±1.04	7.54±2.48	7.23±2.17
24-29		1.03±0.48	2.01±0.52	0.94±0.29	5.58±0.99	5.71±1.01

Table V: Weighted mean abundances (ind m^{-3}) of live and dead *Arctodiaptomus salinus* in 0-15 m water column and at trap depth, 12-15 m, in Lake Shira. For *m* calculations, data on 19, 21, 24, 26, 29 June were used (in bold).

Date in June	0-15 m		12-15 m		$\bar{y}_i - y_i^*$	$y_i^*/\bar{y}_i$
	Live ($\bar{N}_i$)	Dead ($\bar{y}_i$)	Live (N^*)	Dead (y_i^*)		
Nauplii						
19	23885	2056	244	127	1929	0.06
20	nd	nd	42	207	nd	nd
21	33158	2202	1672	212	1990	0.10
24	16828	502	202	48	454	0.10
26	12642	397	180	53	344	0.13
27	12040	266	488	85	181	0.32
28	10842	433	467	223	210	0.54
29	7733	151	180	16	135	0.11
Mean±SE	-	-	-	-	749±315	0.19±0.07
C1-4						
19	14928	1706	191	64	1642	0.04
20	nd	nd	42	101	nd	nd
21	28535	2658	1592	191	2467	0.07
24	25520	1132	223	85	1047	0.08
26	24625	1098	382	74	1024	0.07
27	28656	1251	1295	234	1017	0.19
28	45775	2286	1964	732	1554	0.32
29	25615	1080	653	128	952	0.12
Mean±SE	-	-	-	-	1386±209	0.13±0.04
C5						
19	7535	284	106	21	263	0.07
20	nd	nd	446	154	nd	nd
21	3094	276	1672	149	127	0.54
24	3180	138	1290	96	42	0.70
26	5429	119	1932	212	-93	1.78
27	4899	94	1274	117	-23	1.25
28	5432	257	1285	138	119	0.54
29	2953	106	956	53	53	0.50
Mean±SE	-	-	-	-	70±43	0.77±0.21
Females						
19	3839	400	42	21	379	0.05
20	nd	nd	53	74	nd	Nd
21	4602	497	876	74	423	0.15
24	2857	154	181	22	132	0.14
26	2966	261	234	32	229	0.12
27	3640	238	287	42	196	0.18
28	4567	223	276	53	170	0.24
29	2714	182	175	16	166	0.09
Mean±SE	-	-	-	-	242±43	0.14±0.02
Males						
19	9668	334	127	21	313	0.06
20	nd	nd	64	91	nd	Nd
21	13227	737	1274	53	684	0.07
24	9026	161	154	32	129	0.20
26	7197	191	159	11	180	0.06
27	9622	204	340	42	162	0.21
28	12316	176	541	85	91	0.18
29	6982	207	244	21	186	0.10
Mean±SE	-	-	-	-	249±77	0.13±0.03

Table VI: Values of G, D and NPM (d^{-1}) of *Arctodiaptomus salinus* in Lake Shira calculated from Eq.16 and Eq.17.

Days of June	G_i	D	NPM	
			From Eq.16 (with $\bar{y}_{i}$)	From Eq. 17 (with y_i*)
Nauplii				
19-21	0.473	0.443	0.044	0.006
21-26	0.316	0.285	0.010	-0.009
24-29	0.074	0.067	-0.002	-0.004
C1-4				
19-21	0.592	0.570	0.100	0.034
21-26	0.457	0.424	0.032	-0.008
24-29	0.144	0.133	0.006	0.0001
C5				
19-21	0.234	0.217	0.008	0.0001
21-26	0.117	0.054	0.0003	-0.004
24-29	0.067	0.021	0.001	0.00001
Females				
19-21	0.869	0.823	0.103	0.017
21-26	0.538	0.458	0.048	-0.002
24-29	0.399	0.343	0.023	0.005
Males				
19-21	0.823	0.771	0.049	0.023
21-26	0.516	0.479	0.020	-0.006
24-29	0.408	0.327	0.008	0.002
Population mean				
19-21	-	-	0.061±0.018	- (not calculated)
21-26			0.022±0.008	-
24-29			0.007±0.004	-

Table and Figure Legends

Table I: Major symbols, definitions and their units used in equations and text.

Table II: Number of *Arctodiaptomus salinus* carcasses accumulated in sediment traps per day (Y, ind d^{-1}) and carcass abundances at trap depth, 12-15 m, average of 2-3 samples taken at the beginning and the end of daily trap exposure (y^*_{av}, ind m^{-3}) in Lake Shira (for calculation of v^*) in 2015.

Table III: Number of *Gammarus lacustris* (ind. $sample^{-1}$) in the water column at trap depth and inside the traps in Lake Shira in 2015; dash – no samples.

Table IV: In situ sinking velocity (v^*, m d^{-1}) of *Arctodiaptomus salinus* carcasses calculated from Eq. 4 using data from Table 1 for Lake Shira.

Table V: Weighted mean abundances (ind m^{-3}) of live and dead *Arctodiaptomus salinus* in 0-15 m water column and at trap depth, 12-15 m, in Lake Shira. For *m* calculations, data on 19, 21, 24, 26, 29 June were used (in bold).

Table VI: Values of *G, D* and NPM (d^{-1}) of *Arctodiaptomus salinus* in Lake Shira calculated from Eq.16 and Eq.17.

Fig. 1. Schematic of the sediment trap with digital video recorder and mooring system. Overbar denotes averaging of value over the layer 0 … h, asterisk denotes a value at depth h.

Fig. 2.(A) Wind speed, and current velocity at 14 m depth; (B) isotherms during the study period; (C) mean vertical profiles of temperature, salinity and density; (D) Vertical profile of the turbulent exchange coefficient K_Z.

Fig. 3. Vertical distribution of live and dead *Arctodiaptomus salinus* inLake Shira on 21, 24 and 29 June 2015. The shaded panels correspond to the nighttime.

Fig. 4. Number (as 10-min average) of Arctodiaptomus salinus in the sediment trap detected by the video recorder on 21 June (nighttime) and 27 June (daytime). The numbers in the inserts mark animals visible within the field of view.

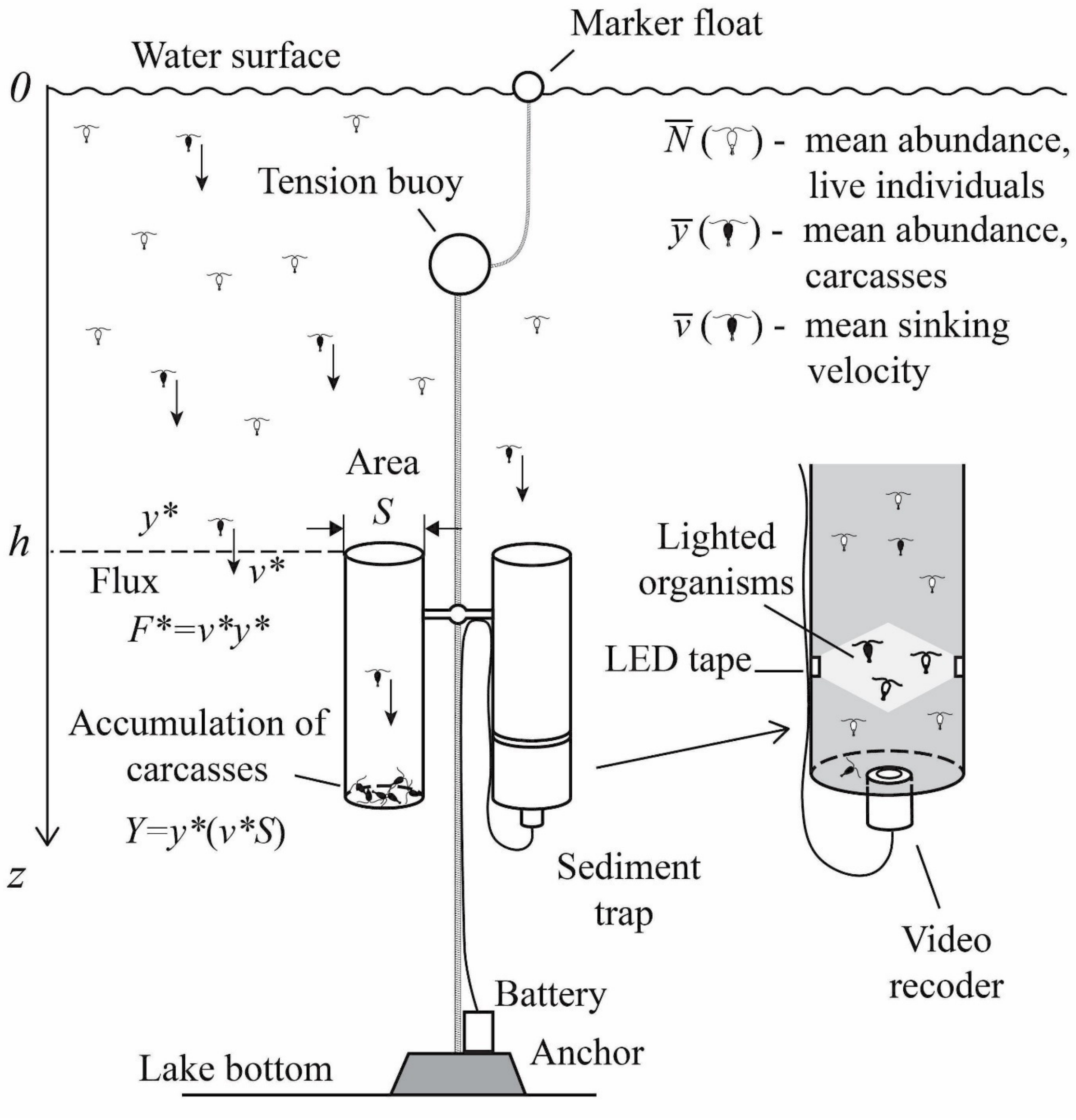
Marker float
Water surface
0
$\overline{N}$ - mean abundance, live individuals
$\bar{y}$ - mean abundance, carcasses
$\bar{v}$ - mean sinking velocity
Tension buoy
Area
S
y*
h
v*
Flux
F*=v*y*
Accumulation of carcasses
Y=y*(v*S)
z
Lighted organisms
LED tape
Sediment trap
Video recoder
Battery
Anchor
Lake bottom

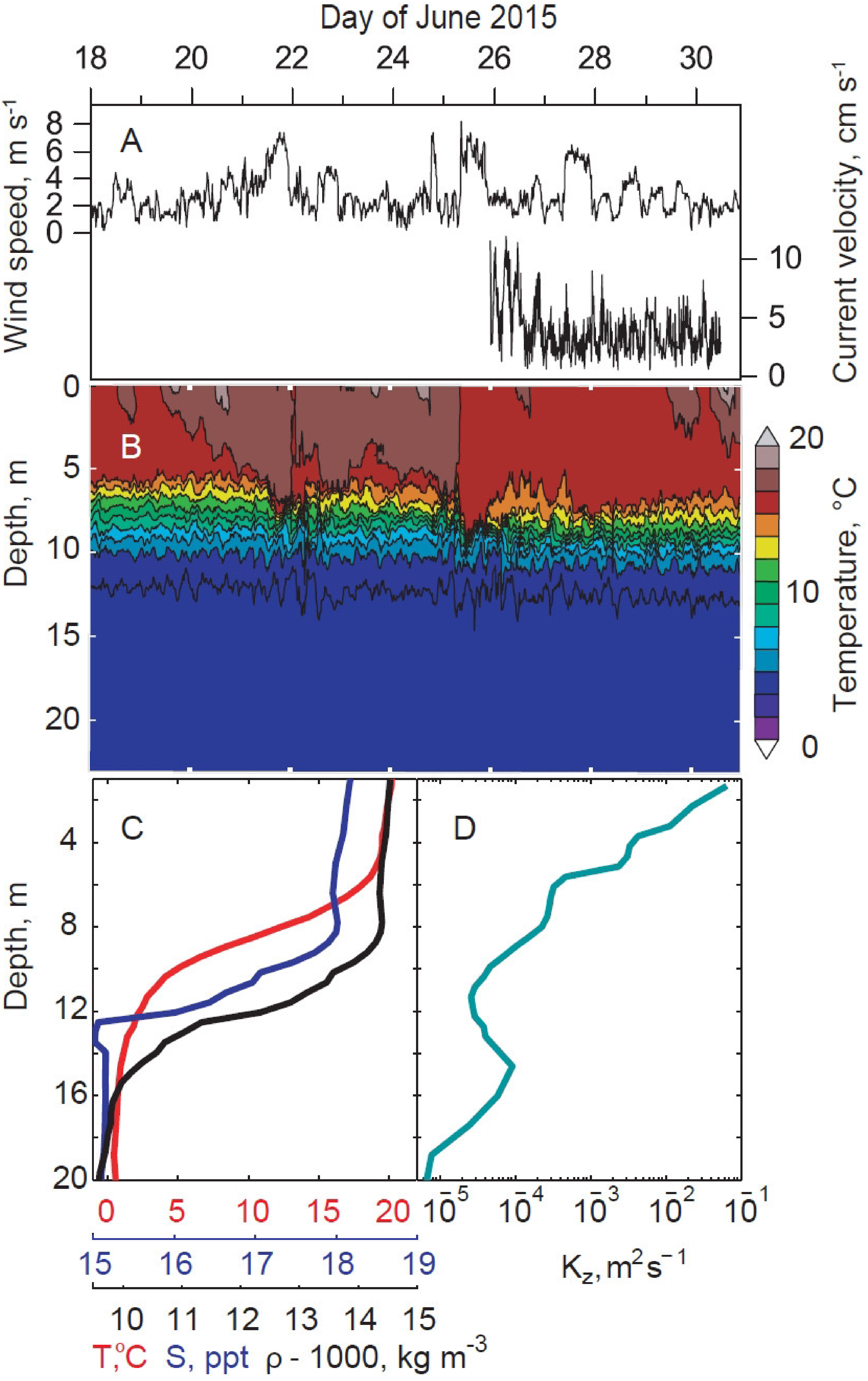
Day of June 2015
18
20
22
24
26
28
30
A
Wind speed, m s^{-1}
8
6
4
2
0
Current velocity, cm s^{-1}
10
5
0
B
Depth, m
0
5
10
15
20
Temperature, °C
20
10
0
C
Depth, m
4
8
12
16
20
0
5
10
15
20
15
16
17
18
19
10
11
12
13
14
15
T,°C
S, ppt
ρ - 1000, kg m^{-3}
D
10^{-5}
10^{-4}
10^{-3}
10^{-2}
10^{-1}
K$_z$, m^{2}s^{-1}

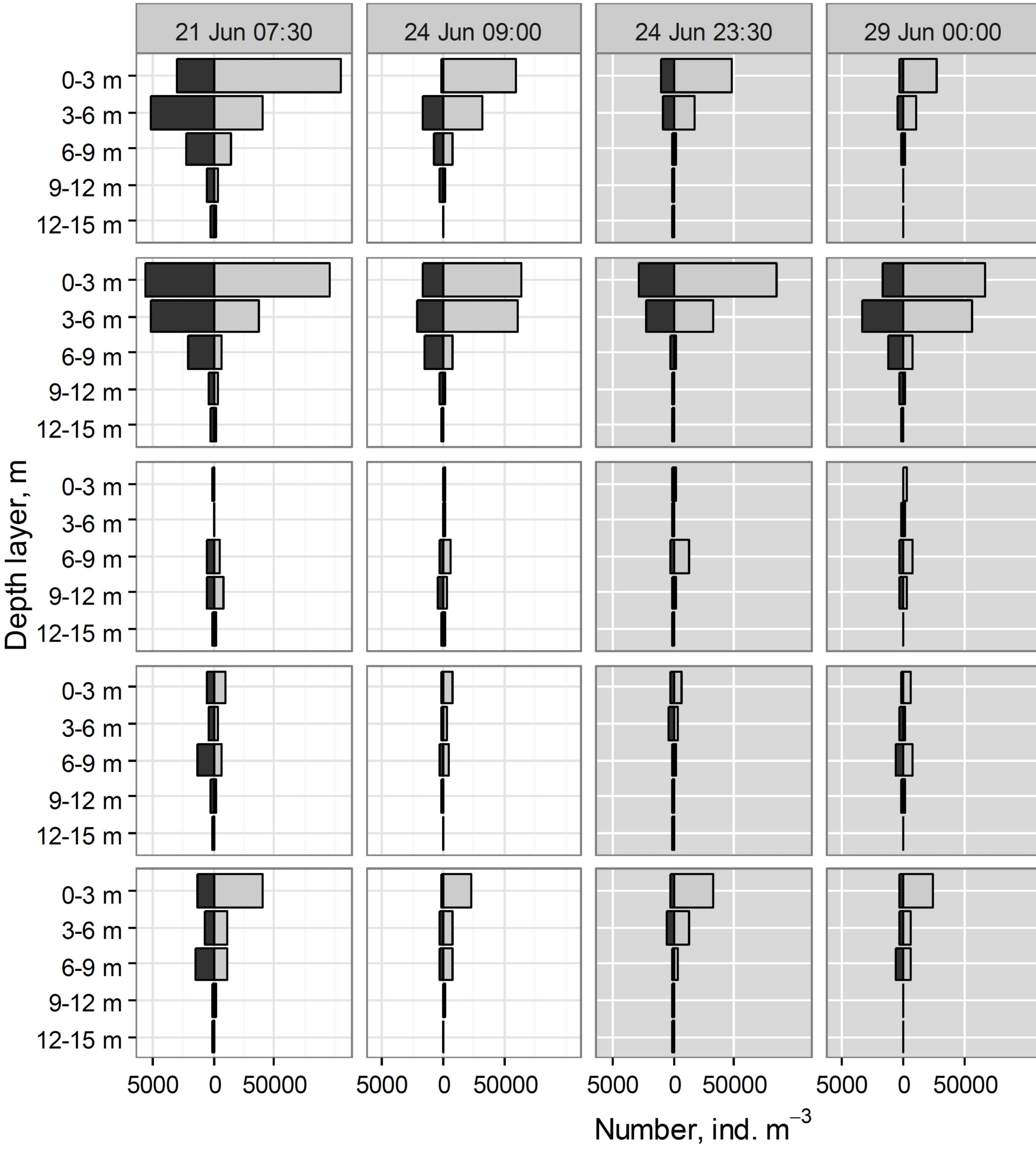
21 Jun 07:30
24 Jun 09:00
24 Jun 23:30
29 Jun 00:00
0-3 m
3-6 m
6-9 m
9-12 m
12-15 m
Depth layer, m
5000
0
50000
Number, ind. m^{-3}

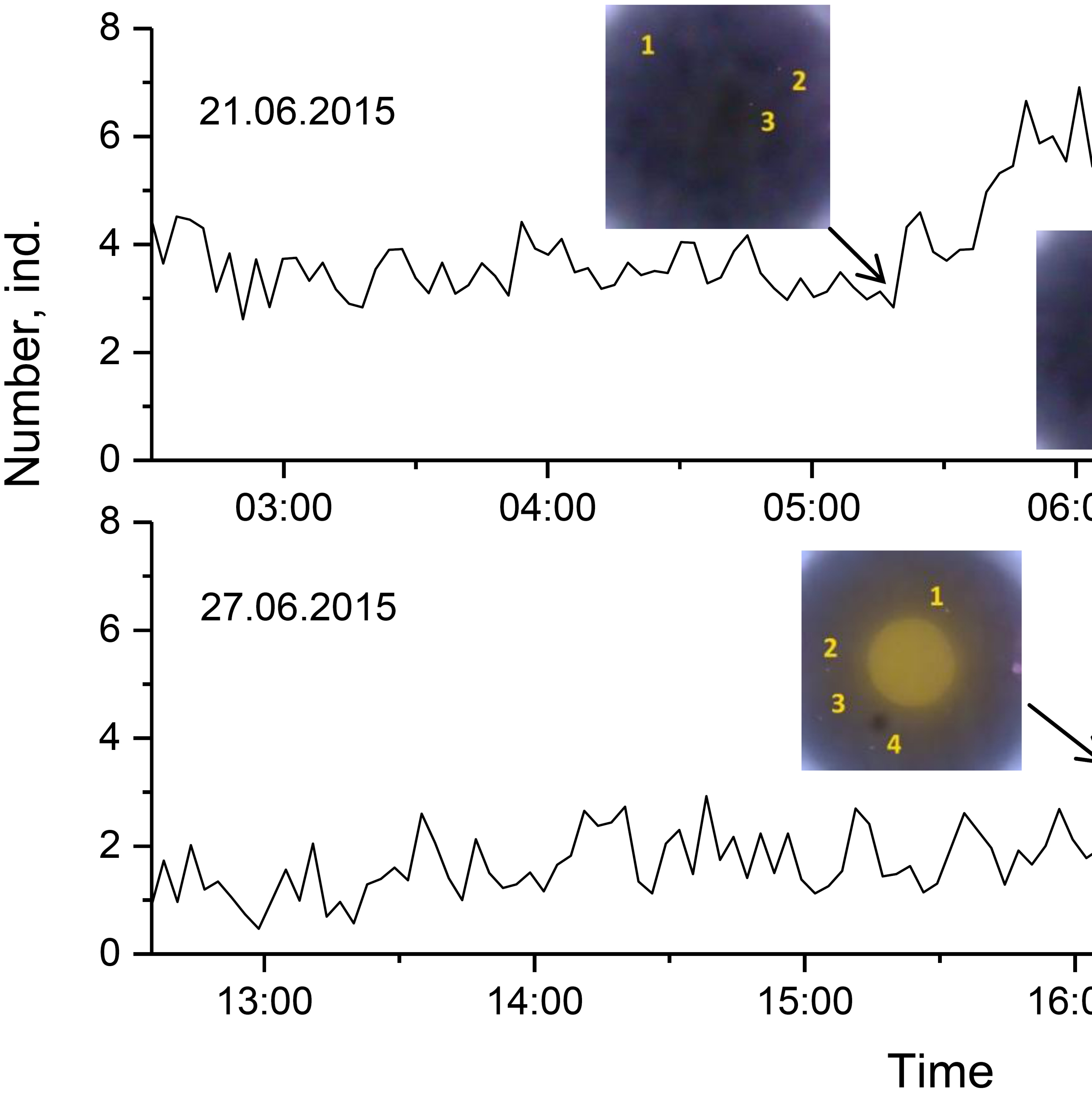
21.06.2015
27.06.2015
Number, ind.
Time
0
2
4
6
8
03:00
04:00
05:00
06:0
13:00
14:00
15:00
16:0
1
2
3
1
2
3
4